arXiv:2605.24938v1 [cs.IR] 24 May 2026

Your Embedding Model is SMARTer Than You Think

Jianrui Zhang*
UW-Madison
harrisz@cs.wisc.edu

Hyun Jung Lee*
Korea University
hyulee@korea.ac.kr

Sukanta Ganguly
NetApp, Inc.
sukanta.ganguly@netapp.com

Tae-Eui Kam
Korea University
kamte@korea.ac.kr

Donghyun Kim†
Korea University
d_kim@korea.ac.kr

Yong Jae Lee†
UW-Madison
yongjaelee@cs.wisc.edu

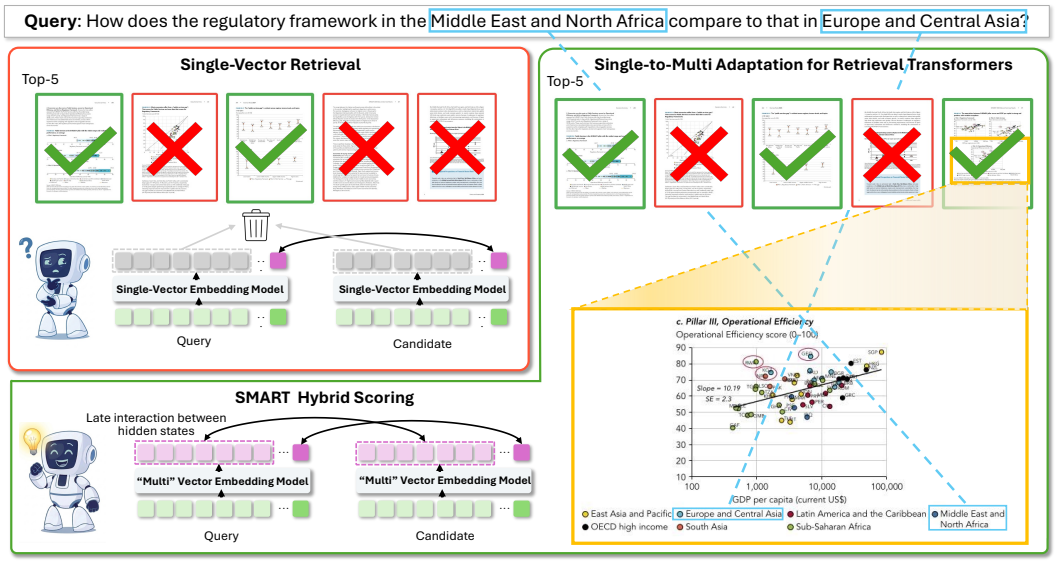

Figure 1: Standard single-vector embedding models (Qwen3-VL-Embedding-8B in this figure) compress sequences into single token representations, which often results in losing local information and underutilizing the remaining hidden states. While existing multi-vector approaches require expensive retraining, SMART reveals that the hidden states of single-vector embedders are **already** geometrically aligned for local matching. SMART thus transforms any single-vector model into a multi-vector variant **both during inference and via lightweight post-training**, the former significantly improving with no training, and the latter allowing us to save time and rival SoTA multi-vector embedders.

Abstract

Multimodal retrieval relies heavily on single-vector retrievers, which compress rich, sequential token sequences into one single global representation. While efficient, they discard fine-grained, local evidence critical for dense retrieval tasks. Multi-vector approaches were introduced as a solution, but they strictly require training and many ignore the necessity of a globally summarizing representation. To address this, we introduce SMART, a framework that unlocks the latent multi-vector capabilities of standard single-vector models. We first demonstrate that standard contrastive training on the pooled embedding implicitly shapes the retrieval geometry of preceding hidden states via gradient flow. By applying direct late-interaction over these frozen hidden states during inference, SMART acts as a plug-and-play

*Equal Contribution
†Equal Advising

Preprint.

upgrade that consistently improves performance across diverse modalities, improving even the state-of-the-art models further on MMEB-V2. We also reveal SMART's superior performance, as simple lightweight post-training not only saves time and compute, but also brings forth further improvement on Visual Document retrieval, allowing a single-vector model to outperform SoTA multi-vector counterparts. Ultimately, SMART offers both a highly efficient inference enhancement and a powerful finetuning technique for multimodal retrieval. We open source our code and weights at `https://github.com/HanSolo9682/SMART`.

1 Introduction

Multimodal Large Language Models (MLLMs) have recently unified dense retrieval across text, images, visual documents, and videos [21, 7]. State-of-the-art (SoTA) systems, such as the Qwen3-VL-Embedding series [10], map these diverse modalities into a highly expressive, shared representation space, enabling efficient global similarity matching. However, these architectures predominantly rely on a single-vector paradigm, collapsing the entire sequence of multimodal hidden states into a single pooling token, such as the end-of-text (`<eot>`) token. While this compression ensures highly efficient indexing and nearest-neighbor search, recent theoretical analyses demonstrate fundamental limitations in its capacity [22, 14, 18]. Since the number of distinct subset rankings a single-vector paradigm can reliably return is strictly bounded by the embedding dimensionality, fine-grained multimodal queries that depend on fine-grained details such as local text, specific visual attributes, or regional bindings can often fail. This is because localized evidence encoded by the transformer can be lost when the input is compressed into the pooled representation used for scoring.

To overcome this expressive bottleneck, researchers have increasingly turned to multi-vector architectures, pioneered in the text domain by ColBERT [8] and recently adapted for multimodal tasks via models like Colpali [3] and jina-embeddings-v4 [4]. Yet, these approaches require either full-scale task-specific finetuning or the introduction of learnable tokens (e.g., MetaEmbed [23]), which incurs significant computational and memory costs during training as they scale quadratically with respect to sequence length. Moreover, methods like Colpali and jina emphasize local token- or patch-level matching without explicitly preserving the global pooled readout that single-vector models use effectively.

To bridge this gap, we introduce SMART (**S**ingle-to-**M**ulti **A**daptation for **R**etrieval **T**ransformers), a framework that converts a single-vector retriever into a multi-vector retriever possible both at inference time and via lightweight finetuning, while preserving its global compatibility signal. We make the observation that the gradients from the contrastive loss on the pooled token propagate through the transformer's computation graph, implicitly organizing the preceding hidden states into a geometry highly compatible with cosine retrieval. SMART initially exploits this by applying an additional late-interaction mechanism (MaxSim) [8] over the pre-pooling hidden states at inference time, combined with the pooled score in a hybrid scoring scheme, effectively recovering localized details without the overhead of training a multi-vector retriever from scratch. Building on this foundation, we further show that lightweight finetuning under the SMART objective yields additional gains, transforming single-vector embedders into competitive multi-vector retrievers. Critically, this conversion saves at least 20% of training time and computation compared to training a multi-vector retriever from scratch under the same recipe.

Our core contributions are as follows:

- We show that single-vector retrievers, despite being trained only with a pooled contrastive objective, **already** retain localized semantic evidence in their non-pooling hidden states. This makes it possible to convert an existing single-vector model into a multi-vector retriever by reusing these hidden states for token-level matching.
- We propose SMART, which can act as a **training-free, plug-and-play** upgrade using our **hybrid scoring** technique. It steadily improves retrieval accuracy across various complex retrieval tasks and backbones, pushing even the SoTA Qwen3-VL-Embedding [10] models to new performance heights.
- We demonstrate that SMART can be further improved with **efficient post-training**, either by attaching a lightweight projection adapter while freezing the pretrained single-vector

backbone, or by finetuning the single-vector embedder with our hybrid scoring objective. These variants enable single-vector embedders to achieve strong multi-vector retrieval performance, saving the time to train a dedicated multi-vector model from scratch.

2 Related Work

Single-Vector Embedding Models Early work on contrastive models (CLIP [17], BLIP [9], SigLIP [25]) and MLLMs [12, 28, 11, 1] paved the way for modern MLLM-based dense retrievers like UniIR [21] and VLM2Vec [7]. Recent advances focus on efficient training strategies (E5-V [6], GME [27]) and highly expressive unified spaces, with Qwen3-VL-Embedding [10] currently achieving SoTA. These approaches, however, waste the compute spent on the local fine-grained non-pooled hidden states. By applying SMART to these off-the-shelf single-vector models, we use that information to demonstrate an easy, training-free approach to convert them into multi-vector architectures for improved retrieval accuracy.

Multi-Vector Embedding Models Because single-vector models face theoretical capacity limits [22], researchers have increasingly turned to multi-vector architectures. Pioneered in text by ColBERT [8], late-interaction mechanisms have been adapted for multimodal tasks via models like Colpali [3], jina-embeddings-v4 [4], and MetaEmbed [23]. Unlike these approaches—which require full-scale task-specific training, adapters, or learnable tokens—SMART can be used entirely inference-only. By combining MaxSim over all hidden states and the global summary token directly to single-vector models, training-free SMART already provides multi-vector performance benefits. On the other hand, lightweight post-training with SMART further improves performance and can convert SoTA single-vector models into SoTA multi-vector while saving time and compute.

Multimodal Retrieval Benchmarks Standardizing evaluation has evolved from foundational baselines like M-BEIR [21] to comprehensive collections like MMEB [7] and MMEB-V2 [15], which span diverse modalities and tasks. Targeted benchmarks have also emerged for specific domains, including ViDoRe [3] and VisRAG [24] for visual documents, Jina-VDR [4] for image retrieval, and UMRB [27] for unified retrieval. In this work, we evaluate SMART on MMEB-V2 due to its broad inclusion of dense retrieval tasks across image, document, and video domains.

3 SMART

In this section, we present SMART, which stands for **S**ingle-to-**M**ulti **A**daptation for **R**etrieval **T**ransformers. We first provide some preliminaries over existing single-vector embedders and their limitations in Sec. 3.1. We then dive into the observation that led to the design of SMART in Sec. 3.2. Lastly, we analyze conditions of applying SMART in Appendix B.

3.1 Preliminaries: Single-vector Objective and Bottleneck

Multimodal embedding models are typically built on rich token-level encoders [10, 15], but they are trained and used through a much narrower readout. Given an input, the encoder produces a sequence of hidden states over text tokens, visual tokens, and special tokens. In standard contrastive training, however, supervision is applied only to a designated pooling representation, most commonly the final-layer hidden state of the end-of-text (`eot`) token. For a query q, a positive candidate c^+, and a set of negatives $\{c^-\}$, the model is optimized with the InfoNCE loss [16]:

$$\mathcal{L} = -\log \frac{\exp\big(s_{\text{single}}(q, c^+)/\tau\big)}{\exp\big(s_{\text{single}}(q, c^+)/\tau\big) + \sum_{c^-} \exp\big(s_{\text{single}}(q, c^-)/\tau\big)}, \tag{1}$$

where the score is computed from the normalized `eot` representations:

$$s_{\text{single}}(q, c) = \big(h^L_{q,\texttt{eot}}\big)^\top h^L_{c,\texttt{eot}}. \tag{2}$$

Thus, although the encoder maintains a full sequence of token-level representations, the training signal directly supervises only the pooled embedding. At retrieval time, the same single-vector readout is used, so each query and candidate is collapsed into one normalized embedding, and ranking reduces to nearest-neighbor search in a shared embedding space.

Single-vector retrieval achieves efficiency by compressing any input into one pooled embedding. This compression induces the *single-vector bottleneck*, where that single representation must support the entire retrieval decision even when relevance heavily depends on localized evidence. This is especially pronounced in fine-grained multimodal retrieval, where details confined to a small portion of the candidate (text or image) are crucial. Consequently, a high single-vector similarity score may indicate aggregate semantic relatedness while completely ignoring localized information. Prior late-interaction and multi-vector retrievers [8, 19, 3, 23] alleviate this limitation by retaining token- or patch-level representations and computing relevance through local interactions. These methods, however, typically require full-scale training, incurring substantial computational and memory costs as self-attention cost grows quadratically with sequence length [20]. This motivates the question: *can we extend an existing single-vector retriever with multi-vector capabilities while preserving its original backbone and efficient pooled representation?*

3.2 Direct Late Interaction over Hidden States

Pooled supervision reaches non-pooling hidden states To approach this question, we examine the supervision dynamics of contrastive retrieval training. At first glance, the contrastive loss in Eq. (1) appears to supervise only the pooled embeddings, suggesting that contrastive training mainly shapes the pooling token. This interpretation overlooks the fact that the pooled state is a function of the full token sequence. Through the transformer's attention and residual pathways, $h^L_{q,\texttt{eot}}$ aggregates information from every non-pooling token, so any token that contributes to the pooled state lies on the gradient path of the contrastive loss:

$$\frac{\partial \mathcal{L}}{\partial h^l_{q,i}} = \left(\frac{\partial z_q}{\partial h^l_{q,i}}\right)^\top \frac{\partial \mathcal{L}}{\partial z_q}, \tag{3}$$

where $h^l_{q,i}$ denotes the hidden state of the i-th query token at layer l, L is the final layer, and z_q is the normalized pooled embedding. This does not mean that each token is supervised as an independent retrieval vector. Rather, although the loss is applied only to the final `eot` representation, this representation is computed from the hidden states of the previous layer through the transformer's attention and residual pathways, so non-pooling hidden states also lie on the gradient path of the pooled contrastive loss. Since the contrastive objective is itself defined by cosine similarity, this indirect supervision encourages the hidden states to organize in a way that supports cosine-based token-level retrieval, even though they are not explicitly trained as standalone retrieval vectors.

Single-to-Multi Adaptation for Retrieval Transformers Motivated by this, we propose SMART, a single-to-multi adaptation that reuses the hidden states of a single-vector retriever for additional token-level retrieval. In its most basic form, this adaptation can be applied even without training a new multi-vector retriever. We keep the original backbone and pooled readout, and add a token-level late-interaction readout over the hidden states already produced by the model.

Importantly, we use this token-level signal as a complement to the original pooled score, not as a replacement. The pooled score captures global query-candidate compatibility, while token-level matching can expose local evidence that may be compressed away by the pooled readout. To combine these two signals without an additional projection or rescaling step, we use final-layer non-pooling hidden states for the token-level readout. We use the final layer rather than earlier layers because the pooled embedding is read out from this layer, making it most directly compatible with the original single-vector scoring space. Note that this is not a claim that earlier layers lack useful information, as they may encode rich lexical, visual, and local details, also as demonstrated in Section 4.6.

Let M_q and M_c denote the valid non-pooling token indices of query q and candidate c, respectively, excluding padding tokens and the pooling token. For each token, we use the normalized final-layer hidden state $\tilde{h}^L_{x,i} = h^L_{x,i}/\|h^L_{x,i}\|_2$. We compute a MaxSim late-interaction score [8] by matching each query token to its most similar candidate token:

$$s_{\text{late}}(q,c) = \frac{1}{|M_q|} \sum_{i \in M_q} \max_{j \in M_c} \tilde{h}^{L\top}_{q,i} \tilde{h}^L_{c,j}. \tag{4}$$

The late-interaction score measures local query coverage in the candidate hidden states. Since it is computed in the same final-layer cosine geometry as the pooled readout, SMART combines it with

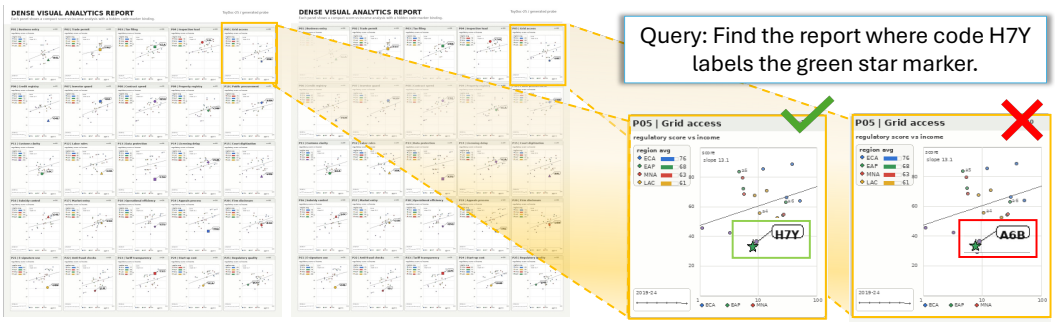

Figure 2: Controlled local-evidence toy benchmark. Each query specifies a local code–marker binding. The hard negative has the same layout, codes, colors, and shapes as the positive report, but the codes are reassigned so that no code remains paired with its original marker.

the original single-vector score by simple addition:

$$s_{\text{hybrid}}(q, c) = s_{\text{single}}(q, c) + s_{\text{late}}(q, c). \tag{5}$$

We use unit weighting to keep SMART hyperparameter-free. Since both terms are cosine-based scores computed from normalized vectors in the same final-layer space, we found simple addition effective across backbones. A candidate ranks highly under s_{hybrid} when it is both globally compatible with the query and locally supported by token-level evidence. While SMART can be applied at inference time without any training, we also explore using s_{hybrid} as the training objective in Appendix D, where we demonstrate how training with hybrid scoring provides the most performance gain.

4 Experiments

In this section, we conduct experiments and analyses using SMART in both inference-only and training scenarios. We first use a controlled experiment to validate our hypothesis of using local evidence for retrieval in Section 4.1. We then show inference-only results in Section 4.2, results of training a SMART adapter in Section 4.3, and results of training and converting our own models in Section 4.4. We then conduct qualitative analysis over some visualizations of SMART in Section 4.5. Lastly, we conduct per layer analysis in Section 4.6.

4.1 Controlled Local-Evidence Toy Benchmark

To make the local-evidence bottleneck of pooled single-vector retrieval explicit, we construct a controlled pairwise benchmark over dense visual reports. As shown in Figure 2, each example consists of a positive report d_A and a hard negative d_B, both rendered as a 5×5 grid of chart panels. Each panel contains one local binding between an alphanumeric code and a visual marker described by color and shape. The hard negative preserves the same document layout, the same set of codes, and the same set of marker descriptors, but applies a no-fixed-point permutation to the code assignments. Thus, for every query, the negative report contains both the queried code and the queried marker descriptor, but not their correct local binding. Because the two reports contain the same global inventory of elements, success depends on recognizing the local pairing between the queried code and marker rather than detecting whether either element appears somewhere in the report.

We generate 40 report pairs with 25 bindings per pair, yielding 1000 queries. Each query ranks only its corresponding positive and hard-negative reports, and we report pairwise accuracy. The original single-vector score selects the positive report for only 31.9% of queries, showing that the pooled single-vector readout is unreliable when relevance is determined by a specific local binding. Replacing the single score with a late-interaction score over final-layer non-pooling hidden states improves accuracy to 56.8%, showing that these hidden states expose local code–marker binding evidence that is not reliably accessible through the pooled readout. The gap between these scores suggests that the bottleneck lies in the pooled single-vector readout rather than in the absence of local information in the model. When the retrieval decision depends on a specific code–marker binding, the pooled score does not reliably capture the evidence needed to distinguish the positive report from the hard negative. In contrast, late interaction over non-pooling hidden states makes part of this local evidence available for scoring.

Table 1: Average per-task performance on MMEB-V2. We report Recall@1 for image and video retrieval tasks and NDCG@5 for visual document retrieval tasks. Applying training-free SMART achieves consistent improvement over all dense retrieval tasks and generalizes across different backbones, including the SoTA Qwen3-VL-Embedding series.

Model	**Image**	**Visdoc**				**Video**	**Average**
	RET	VDRv1	VDRv2	VR	OOD	RET	
# Tasks	12	10	4	6	4	5	
VLM2Vec-V2.0 [15]	69.50	75.34	47.28	79.43	62.04	28.66	64.50
+ SMART	**69.95**	**80.23**	**51.08**	**82.76**	**64.00**	**30.03**	**67.04**
GME-2B [27]	70.13	87.61	53.76	82.49	66.93	26.73	69.00
+ SMART	**71.05**	**87.97**	**57.23**	**84.18**	**67.82**	26.50	**70.00**
GME-7B [27]	73.09	90.01	60.43	86.20	69.22	29.92	72.26
+ SMART	**73.57**	**90.12**	**61.04**	**87.05**	**69.43**	29.38	**72.56**
Qwen3-VL-Embed-2B [10]	74.91	84.46	65.38	86.19	69.37	54.04	74.87
+ SMART	**75.33**	**85.52**	**66.61**	**86.87**	**69.90**	**56.05**	**75.77**
Qwen3-VL-Embed-8B [10]	80.09	87.29	69.35	88.78	73.27	59.01	78.83
+ SMART	**80.15**	**87.92**	**70.57**	**89.12**	73.21	**60.43**	**79.34**

Combining the two scores yields 42.6%. Although this is lower than late interaction alone and below chance, this behavior is expected in this adversarially controlled setting and should not be interpreted as evidence against the hybrid scoring objective used in natural retrieval settings. The original pooled score is already below chance on this benchmark, so adding it to the late-interaction score does not act as a neutral global prior. Instead, it reintroduces a signal based on aggregate document similarity, while the retrieval decision depends only on whether the queried code and marker are correctly bound. Since the positive and hard negative share the same layout, codes, colors, and shapes, this aggregate signal can be systematically misaligned with the local-binding decision and can weaken the late-interaction signal when the two are combined. We therefore report the hybrid score here to characterize this diagnostic stress test, whereas the subsequent retrieval experiments evaluate SMART in settings where global compatibility remains informative and can complement local evidence.

We further compare against native multi-vector retrievers in the same pairwise setting. Late-interaction retrieval with Qwen3-VL-Embedding-2B's hidden states (56.8%) outperforms both jina-embeddings-v4 multi-vector retrieval (50.9%) and Colpali (48.7%). Both native baselines perform near chance, underscoring how challenging the local-binding setting is even for retrievers explicitly designed for token-level matching. These results should not be read as evidence that hidden-state scoring is universally preferable. Rather, the benchmark is deliberately constructed to remove useful global cues and focus the evaluation on local binding evidence. Under this controlled setting, the result supports our central motivation that the pooled single-vector score can miss local evidence needed for retrieval, while the non-pooling hidden states of the same model can still expose that evidence through late interaction. Further generation details are provided in Appendix A.

4.2 Inference-Only Results: SMART's Plug-and-Play Effectiveness

Table 1 presents the comprehensive evaluation of inference-only SMART across dense retrieval tasks within the MMEB-V2 [15] benchmark (Apache-2.0 License). We note reasons for selecting these tasks in Appendix B. The results clearly demonstrate that SMART yields substantial, consistent, and broad-based performance improvements across diverse retrieval domains.

Most remarkably, these consistent performance gains are achieved entirely *inference-only*. Without requiring a single step of additional parameter updates or costly finetuning, SMART effectively unlocks the latent representational power of existing models. This shows that SMART can be a highly efficient, plug-and-play upgrade for modern multimodal retrieval pipelines.

Universal Compatibility Across Backbones. An important feature of SMART is its robust generalizability across different models. SMART greatly boosts performance of baselines like VLM2Vec-V2.0, driving an overall average improvement of +2.54%. Furthermore, SMART's efficacy is not limited to weaker baselines; it scales well to highly optimized, SoTA architectures. When ap-

Table 2: Results of training SMART adapters when evaluated on MMEB-V2's visdoc subset. In the SMART columns, ✓denotes SMART hybrid scoring s_{hybrid}. ✗$_s$ denotes no SMART with single-vector scoring only, while ✗$_m$ denotes no SMART with late-interaction/multi-vector scoring only. ✓† means freezing the model and only training an s_{late} adapter.

Model	Size	SMART		Visdoc				Average
		Train	Eval	VDRv1	VDRv2	VR	OOD	
SoTA Single-Vector Embedders (Qwen3-VL-Embedding Family)								
Qwen3-VL-Embedding	2B	✗$_s$	✗$_s$	84.60	65.33	86.34	69.27	79.27
		✗$_s$	✓	85.52	66.61	86.87	69.90	80.10
		✓†	✓	**87.09**	**67.08**	**87.99**	**70.73**	**81.25**
	8B	✗$_s$	✗$_s$	87.29	69.35	88.78	73.27	82.33
		✗$_s$	✓	87.92	70.57	89.12	73.21	82.88
		✓†	✓	**89.42**	**71.25**	**89.67**	**73.99**	**83.89**
SoTA Multi-Vector Embedders								
Colpali-1.3 [3]	3B	✗$_m$	✗$_m$	83.60	52.00	81.10	43.10	71.00
jina-embeddings-v4 [4]	4B	✗$_m$	✗$_m$	89.94	57.36	88.74	70.18	80.91

plied to the formidable Qwen3-VL-Embedding series, SMART still extracts consistent gains. On Qwen3-VL-Embedding-2B, we observe nearly a +1.0% average improvement. Even on the larger Qwen3-VL-Embedding-8B, SMART elevates the metrics, raising the SoTA's average from 78.83% to 79.34%.

Robustness Across Retrieval Domains. The granular task breakdown further highlights SMART's versatility. In the complex domain of Visual Document Retrieval (Visdoc; VDRv1, VDRv2, VR, and OOD subsets), where fine-grained text-to-visual alignment is particularly important, the addition of SMART demonstrates consistent improvements across all four tested backbones.

Similarly, in Video Retrieval, SMART also proves to be highly adept, securing substantial boosts for VLM2Vec (+1.37%), Qwen3-VL-Embedding-2B (+2.01%), and Qwen3-VL-Embedding-8B (+1.42%). We gray out GME because it is not trained to handle multiple frames, and thus when only the middle frame is provided (as was done in MMEB-V2 [15]), we see minimal change.

In summary, the empirical evidence underscores SMART as a highly versatile, zero-training-cost enhancement that significantly elevates the retrieval ceiling for single-vector multimodal backbones it is paired with.

4.3 Lightweight Adapter Post-Training

The previous section established SMART as an effective plug-and-play upgrade. We next investigate whether late interaction can benefit from a minimally learned readout. Integrating SMART into lightweight post-training allows us to explicitly optimize the non-pooling-token hidden states for late interaction, capitalizing on the foundation laid by the inference-only gains.

To isolate the effect of the readout, we keep the embedder frozen and train only a token-wise linear adapter on top of the final-layer hidden states. For each valid hidden state $h_i^L \in \mathbb{R}^H$, the adapter applies layer normalization followed by a linear projection and ℓ_2 normalization:

$$r_i = \text{normalize}\big(\text{Linear}\big(\text{LN}(h_i^L)\big)\big)\,, \tag{6}$$

where $\text{Linear} : \mathbb{R}^H \to \mathbb{R}^d$ is the only trainable readout module. We use the Colpali [3] training set with global batch size 512. Training is very efficient as the adapter for Qwen3-VL-Embedding-2B only takes 1 hour and 50 minutes on one node of eight 48GB A6000s. We replace the normalized hidden states in Eq. (4) with the adapted token vectors r_i while keeping the pooled single-vector score unchanged and apply the same hybrid scoring as Eq. (5). The adapter is trained only with s_{late}.

This readout-only adapter improves over the training-free SMART variant across both model sizes, as demonstrated in Table 2. We see an impressive 1-point gain on both the 2B and 8B Qwen3-VL-Embedding variants, noting that the 8B model has doubled the gain from inference-only SMART

Table 3: Results of training and converting single-vector models when evaluated on the visdoc subset. ✗$_s$ denotes no SMART with single-vector scoring only, while ✗$_m$ denotes no SMART with late-interaction/multi-vector scoring only. ✓denotes SMART hybrid scoring s_{hybrid} and ✓† means extended training (*not* from scratch) with LoRA using s_{hybrid}.

Model	**Training Time**	**SMART**		**Visdoc**				**Average**
		Train	Eval	VDRv1	VDRv2	VR	OOD	
Our Trained Embedders (LamRA-Ret Family)								
LamRA-Single	6.5 hours	✗$_s$	✗$_s$	81.58	50.72	78.41	63.50	72.60
LamRA-Single-SMART	6.5 hours	✗$_s$	✓	83.02	52.25	80.52	64.50	74.18
LamRA-Single-Convert	**9.5 hours**	✓†	✓	86.93	54.60	84.39	67.61	77.68
LamRA-Multi	12 hours	✗$_m$	✗$_m$	87.93	54.29	85.24	67.91	78.31

($\sim$0.5) to the SMART adapter. The consistent gain suggests that the frozen backbone already contains local evidence, and that a lightweight token-level readout can make this evidence more compatible with late interaction.

Most importantly, we find that **Qwen3-VL-Embedding-2B is able to outperform the SoTA multi-vector embedding model jina-embeddings-v4** by a 0.34-point margin with the help of the SMART adapter. We emphasize that converting the model to a SoTA multi-vector embedder was done with only 1 hour and 50 minutes of training using academia-level resources. This shows how simple and efficient it is to transform a single-vector model to a multi-vector one using SMART.

4.4 Efficient Conversion via LoRA Finetuning with SMART

From Table 2, we see how the multi-vector model jina-embedding-v4 outperforms the SoTA 2B single-vector retriever (original, without SMART). Thus, one may ask, "Why would one not simply train a multi-vector model from scratch for better performance?" To truly test the effectiveness of SMART, we seek to answer that question by training our own single- and multi-vector embedders.

We adopt the LamRA-Ret recipe [13] to finetune the backbone Qwen3-VL-2B-Instruct [2] (the same starting model as Qwen3-VL-Embedding-2B). All training is done on one node of eight 80GB A100s with global batch size 512, using LoRA [5] with $r = 128$, $\alpha = 256$, cosine annealing scheduling with max learning rate $1e-4$ and a warmup ratio of 0.03. We only train on the Colpali [3] training set for 4 epochs for LamRA-Single and LamRA-Multi, while for LamRA-Single-Convert we trained on top of LamRA-Single for only one more epoch.

The results are shown in Table 3. The first model, LamRA-Single, is trained only using the s_{single} objective and takes 6.5 hours. When we compare the baseline single-vector model to the inference-only application of SMART (Rows 1 and 2), we observe a solid $\sim$1.6-point average improvement (72.60 to 74.18), consistent with the training-free boosts established in Section 4.2.

Comparing Rows 3 and 4 highlights the effectiveness and efficiency of using SMART. In Row 3, we start from the LamRA-Single checkpoint, and apply the exact same recipe but only train for one more epoch, this time using the s_{hybrid} objective, and take an extra 3 hours (9.5 hours in total) to train LamRA-Single-Convert. We also train another model, LamRA-Multi, from the Qwen3-VL-2B-Instruct model, only using the s_{late} objective, which takes 12 hours. We see both models perform significantly better than the Single variants. Yet, more importantly, the converted model takes significantly shorter to train in total ($\sim 20\%$) while performing only slightly behind the Multi variant (~ 0.63). Thus, our answer to the question is: **Using SMART to convert a single-vector model into a multi-vector model is more efficient than training one from scratch without significant loss of performance.**

4.5 Qualitative Analysis

SMART is designed to complement the global signal of a single-vector retriever with token-level evidence from hidden states. We qualitatively examine this complementarity on examples in Figures 1 and 3 to illustrate how the pooled score can retrieve a globally similar but incorrect candidate, while the late-interaction signal helps recover local visual details that support the correct match. We include more visualization analyses in Appendix C.

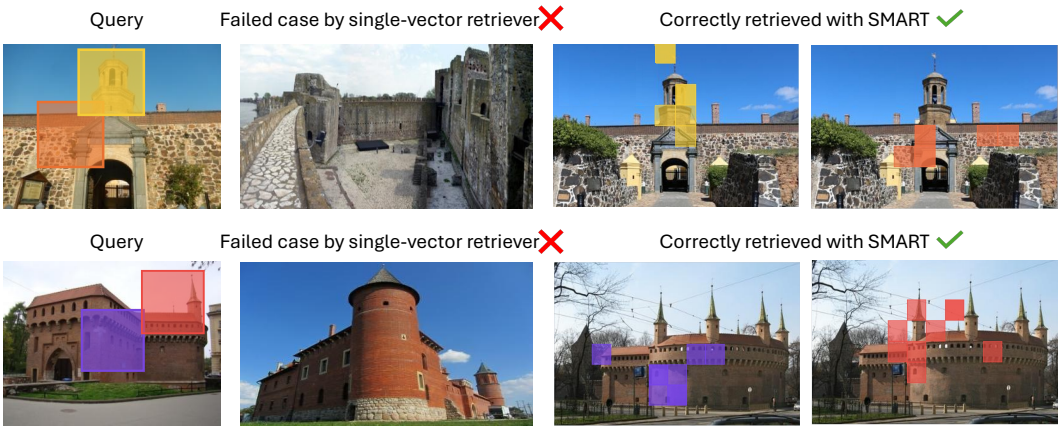

Figure 3: Qualitative visualization of SMART on image-to-image retrieval. Each row shows the query, a failed result from the original single-vector retriever, and the correct result retrieved by SMART. Colored boxes visualize the local evidence used by SMART. Each selected query patch is matched to the highest-similarity candidate patch under the MaxSim late-interaction score, with matching colors denoting the corresponding query-candidate pair. These localized matches help SMART recover details that are often obscured by global single-vector compression.

Figure 1 demonstrates a scenario where a SoTA multimodal retrieval model, Qwen3-VL-Embedding-8B, fails to retrieve one of three relevant images for a query in the Vidore Economic Reports task (from the MMEB-V2 Visual Document subset). However, the application of SMART successfully corrects this failure. A closer examination of the visual content reveals fine-grained details within a chart legend (specifically, the labels "Europe and Central Asia" and "Middle East and North Africa") which align perfectly with the query text. This highlights a fundamental limitation of single-vector models: they often fail to capture granular details because they compress the entire document into a single, global representation optimized for broad comparisons across diverse queries and corpora. In contrast, SMART effectively recovers this localized information.

Furthermore, Figure 3 shows that the original single-vector retriever can select globally plausible but incorrect candidates. These errors are natural under a pooled representation, as the retrieved images often share the same broad visual category, such as castles, fortresses, towers, or stone architecture, but differ in the specific local structures needed to identify the correct instance. The visualization further shows where SMART obtains its token-level evidence. For selected query tokens, we highlight the candidate-image token with the highest hidden-state cosine similarity, which is exactly the token selected by the MaxSim operation in s_{late}. These highlighted regions concentrate on small, semantically meaningful parts of the candidate image rather than spreading uniformly, indicating that individual query tokens match specific local regions instead of averaged global content. Such localized cues can be obscured by the pooled readout when the entire candidate is summarized into a single embedding.

4.6 Layer-wise Late Interaction Analysis

Finally, we investigate the layer-wise dynamics of late interaction in Qwen3-VL-Embedding-2B by comparing two distinct configurations. On the left side of Table 4, we pair the pooled representation (e.g., the `<eot>` token) of a given Layer X with its own corresponding hidden states. This reveals an almost strictly upward trajectory in retrieval performance as we progress to deeper layers, demonstrating that the model progressively builds more effective and discriminative representations for matching.

Conversely, on the right side of the table, we hold the global anchor fixed using the highly contextualized pooled vector from the final layer (Layer 28) as is defined by their training objective, while varying the intermediate layer X that provides the hidden states for late interaction. This setup strongly highlights the inherent robustness of the single final-layer vector, which maintains an exceptionally high baseline score even when paired with hidden states from much earlier in the network. Furthermore, this analysis demonstrates that when anchored by the Layer 28 `<eot>` token,

Table 4: Layer-wise analysis on visual-document retrieval tasks. We compare using the same layer X for both pooled and token-level readouts with keeping the original last-layer pooled score fixed while varying only the hidden layer X used for late interaction.

X	X-th Layer Pooling					Last Layer Pooling				
	VDRv1	VDRv2	VR	OOD	Average	VDRv1	VDRv2	VR	OOD	Average
4	56.77	25.53	57.93	37.18	48.59	84.90	64.94	86.66	69.31	79.42
8	72.94	39.25	69.87	47.28	62.28	85.20	66.01	87.00	69.44	79.83
12	75.04	42.40	70.44	52.94	64.77	85.08	65.64	86.76	69.51	79.67
16	71.46	40.22	63.30	50.43	60.71	85.06	65.90	86.70	69.63	79.70
20	80.45	55.01	78.34	60.40	72.34	**85.56**	66.42	**87.19**	69.87	**80.16**
24	82.68	60.93	83.41	64.99	76.29	85.31	66.41	87.16	69.80	80.04
28	**85.52**	**66.61**	**86.87**	**69.90**	**80.10**	85.52	**66.61**	86.87	**69.90**	80.10

strictly utilizing hidden states from Layer 28 is not an absolute requirement for peak performance. In fact, utilizing hidden states from Layer 20 yields an average score of 80.16, which does not perform significantly better than the 80.10 achieved with Layer 28. This observation validates the flexibility of a hybrid approach: the final-layer single vector serves as highly robust standalone anchor, while the broader late-layer region (especially Layer 20 and beyond) successfully encodes rich, fine-grained information that seamlessly aids the single vector to maximize retrieval accuracy.

5 Conclusion

In this work, we introduced SMART (Single-to-Multi Adaptation for Retrieval Transformers) to overcome the fundamental information bottleneck inherent in single-vector multimodal retrieval models. By demonstrating that contrastive training on a global pooling token implicitly structures the preceding hidden states for retrieval, we successfully unlocked these localized representations using a late-interaction MAXSIM operator and our special hybrid scoring objective.

Our extensive experiments highlight SMART's dual utility as both a highly effective inference-time enhancement and an efficient training paradigm. In an inference-only setting, SMART functions as a zero-training-cost, plug-and-play upgrade that consistently improves accuracy across diverse modalities, scaling robustly to SoTA architectures like the Qwen3-VL-Embedding series. Crucially, when training only lightweight auxiliaries, SMART further improves performance by explicitly optimizing the non-pooling-token hidden states for late interaction together with the global summary token, allowing us to convert a SoTA single-vector embedding model into a multi-vector variant better than SoTA pretrained counterparts.

Ultimately, SMART provides a robust, computationally efficient pathway for recovering fine-grained, localized evidence from existing multimodal architectures, raising the ceiling for universal dense retrieval systems.

Limitations

This work focuses on dense retrieval tasks, as we find SMART not beneficial when used as an inference-only tool for more global tasks like classification. Due to limited compute, we could only train our LamRA-Ret models on the visdoc subset. We leave the exploration of these aspects as valuable future work.

Acknowledgments

This work was supported in part by NSF IIS2404180, Institute of Information & communications Technology Planning& Evaluation (IITP) grants (MSIT) (No. 2022-0-00871, Development of AI Autonomy and Knowledge Enhancement for AI Agent Collaboration), (No. RS-2025-2543949. Environment-Aware and Domain-Adaptive Multimodal Embodied AI for Real-World Interaction), the Artificial Intelligence Graduate School Program at Korea University (No. RS-2019-II190079) and grant No. RS-2025-25439490, the National Research Foundation of Korea (NRF) grant funded

by the Korea government (MSIT) (RS-2025-25302986); and Culture, Sports and Tourism R&D Program through the Korea Creative Content Agency grant funded by the Ministry of Culture, Sports and Tourism in 2024 (Project Name: International Collaborative Research and Global Talent Development for the Development of Copyright Management and Protection Technologies for Generative AI, Project Number: RS-2024-00345025).

References

[1] Jinze Bai, Shuai Bai, Shusheng Yang, Shijie Wang, Sinan Tan, Peng Wang, Junyang Lin, Chang Zhou, and Jingren Zhou. Qwen-vl: A versatile vision-language model for understanding, localization, text reading, and beyond. *arXiv preprint arXiv:2308.12966*, 2023.

[2] Shuai Bai, Yuxuan Cai, Ruizhe Chen, Keqin Chen, Xionghui Chen, Zesen Cheng, Lianghao Deng, Wei Ding, Chang Gao, Chunjiang Ge, et al. Qwen3-vl technical report. *arXiv preprint arXiv:2511.21631*, 2025.

[3] Manuel Faysse, Hugues Sibille, Tony Wu, Bilel Omrani, Gautier Viaud, CELINE HUDELOT, and Pierre Colombo. Colpali: Efficient document retrieval with vision language models. In *International Conference on Learning Representations*, pages 61424–61449, 2025.

[4] Michael Günther, Saba Sturua, Mohammad Kalim Akram, Isabelle Mohr, Andrei Ungureanu, Bo Wang, Sedigheh Eslami, Scott Martens, Maximilian Werk, Nan Wang, and Han Xiao. jina-embeddings-v4: Universal embeddings for multimodal multilingual retrieval. *https://arxiv.org/abs/2506.18902*, 2025.

[5] Edward J. Hu, Yelong Shen, Phillip Wallis, Zeyuan Allen-Zhu, Yuanzhi Li, Shean Wang, Lu Wang, and Weizhu Chen. Lora: Low-rank adaptation of large language models. *https://arxiv.org/abs/2106.09685*, 2021.

[6] Ting Jiang, Minghui Song, Zihan Zhang, Haizhen Huang, Weiwei Deng, Feng Sun, Qi Zhang, Deqing Wang, and Fuzhen Zhuang. E5-v: Universal embeddings with multimodal large language models. *https://arxiv.org/abs/2407.12580*, 2024.

[7] Ziyan Jiang, Rui Meng, Xinyi Yang, Semih Yavuz, Yingbo Zhou, and Wenhu Chen. Vlm2vec: Training vision-language models for massive multimodal embedding tasks. *https://arxiv.org/abs/2410.05160*, 2025.

[8] Omar Khattab and Matei Zaharia. Colbert: Efficient and effective passage search via contextualized late interaction over bert. *https://arxiv.org/abs/2004.12832*, 2020.

[9] Junnan Li, Dongxu Li, Caiming Xiong, and Steven Hoi. Blip: Bootstrapping language-image pre-training for unified vision-language understanding and generation. *https://arxiv.org/abs/2201.12086*, 2022.

[10] Mingxin Li, Yanzhao Zhang, Dingkun Long, Keqin Chen, Sibo Song, Shuai Bai, Zhibo Yang, Pengjun Xie, An Yang, Dayiheng Liu, Jingren Zhou, and Junyang Lin. Qwen3-vl-embedding and qwen3-vl-reranker: A unified framework for state-of-the-art multimodal retrieval and ranking. *https://arxiv.org/abs/2601.04720*, 2026.

[11] Haotian Liu, Chunyuan Li, Yuheng Li, and Yong Jae Lee. Improved baselines with visual instruction tuning. In *arXiv*. arXiv:2310.03744, 2023.

[12] Haotian Liu, Chunyuan Li, Qingyang Wu, and Yong Jae Lee. Visual instruction tuning. In *NeurIPS*, 2023.

[13] Yikun Liu, Pingan Chen, Jiayin Cai, Xiaolong Jiang, Yao Hu, Jiangchao Yao, Yanfeng Wang, and Weidi Xie. Lamra: Large multimodal model as your advanced retrieval assistant. *https://arxiv.org/abs/2412.01720*, 2024.

[14] Yi Luan, Jacob Eisenstein, Kristina Toutanova, and Michael Collins. Sparse, dense, and attentional representations for text retrieval. *Transactions of the Association for Computational Linguistics*, 9: 329–345, 2021.

[15] Rui Meng, Ziyan Jiang, Ye Liu, Mingyi Su, Xinyi Yang, Yuepeng Fu, Can Qin, Zeyuan Chen, Ran Xu, Caiming Xiong, Yingbo Zhou, Wenhu Chen, and Semih Yavuz. Vlm2vec-v2: Advancing multimodal embedding for videos, images, and visual documents. *https://arxiv.org/abs/2507.04590*, 2025.

[16] Aaron van den Oord, Yazhe Li, and Oriol Vinyals. Representation learning with contrastive predictive coding. *arXiv preprint arXiv:1807.03748*, 2018.

[17] Alec Radford, Jong Wook Kim, Chris Hallacy, Aditya Ramesh, Gabriel Goh, Sandhini Agarwal, Girish Sastry, Amanda Askell, Pamela Mishkin, Jack Clark, Gretchen Krueger, and Ilya Sutskever. Learning transferable visual models from natural language supervision. *https://arxiv.org/abs/2103.00020*, 2021.

[18] Nils Reimers and Iryna Gurevych. The curse of dense low-dimensional information retrieval for large index sizes. In *Proceedings of the 59th Annual Meeting of the Association for Computational Linguistics and the 11th International Joint Conference on Natural Language Processing (Volume 2: Short Papers)*, pages 605–611, 2021.

[19] Keshav Santhanam, Omar Khattab, Jon Saad-Falcon, Christopher Potts, and Matei Zaharia. Colbertv2: Effective and efficient retrieval via lightweight late interaction. In *Proceedings of the 2022 Conference of the North American Chapter of the Association for Computational Linguistics: Human Language Technologies*, pages 3715–3734, 2022.

[20] Ashish Vaswani, Noam Shazeer, Niki Parmar, Jakob Uszkoreit, Llion Jones, Aidan N Gomez, Łukasz Kaiser, and Illia Polosukhin. Attention is all you need. *Advances in neural information processing systems*, 30, 2017.

[21] Cong Wei, Yang Chen, Haonan Chen, Hexiang Hu, Ge Zhang, Jie Fu, Alan Ritter, and Wenhu Chen. Uniir: Training and benchmarking universal multimodal information retrievers. *https://arxiv.org/abs/2311.17136*, 2023.

[22] Orion Weller, Michael Boratko, Iftekhar Naim, and Jinhyuk Lee. On the theoretical limitations of embedding-based retrieval. *https://arxiv.org/abs/2508.21038*, 2026.

[23] Zilin Xiao, Qi Ma, Mengting Gu, Chun cheng Jason Chen, Xintao Chen, Vicente Ordonez, and Vijai Mohan. Metaembed: Scaling multimodal retrieval at test-time with flexible late interaction. *https://arxiv.org/abs/2509.18095*, 2026.

[24] Shi Yu, Chaoyue Tang, Bokai Xu, Junbo Cui, Junhao Ran, Yukun Yan, Zhenghao Liu, Shuo Wang, Xu Han, Zhiyuan Liu, et al. Visrag: Vision-based retrieval-augmented generation on multi-modality documents. *arXiv preprint arXiv:2410.10594*, 2024.

[25] Xiaohua Zhai, Basil Mustafa, Alexander Kolesnikov, and Lucas Beyer. Sigmoid loss for language image pre-training. *https://arxiv.org/abs/2303.15343*, 2023.

[26] Jianrui Zhang, Anirudh Sundara Rajan, Brandon Han, Soochahn Lee, Sukanta Ganguly, and Yong Jae Lee. Reasoning-augmented representations for multimodal retrieval. *https://arxiv.org/abs/2602.07125*, 2026.

[27] Xin Zhang, Yanzhao Zhang, Wen Xie, Mingxin Li, Ziqi Dai, Dingkun Long, Pengjun Xie, Meishan Zhang, Wenjie Li, and Min Zhang. Gme: Improving universal multimodal retrieval by multimodal llms. *https://arxiv.org/abs/2412.16855*, 2025.

[28] Deyao Zhu, Jun Chen, Xiaoqian Shen, Xiang Li, and Mohamed Elhoseiny. Minigpt-4: Enhancing vision-language understanding with advanced large language models. In *arXiv*, 2023.

A Toy Dataset

The pooling bottleneck is difficult to isolate in natural retrieval benchmarks, where global semantics, local evidence, and dataset biases are often entangled. We therefore construct a controlled toy benchmark that directly tests whether a retriever can distinguish local bindings from aggregate content. The goal of this probe is not to model real documents in full generality, but to create a setting where the single-vector failure mode is unambiguous. Each example consists of a pair of dense visual documents, denoted by (d_A, d_B). Both documents have the same layout: a 5×5 grid of panels, where each panel contains a cluttered chart and one local code–marker binding. A marker is described by a color and a shape, and is labeled by a short alphanumeric code. For each pair, d_A is the positive document. The hard negative d_B preserves the same layout, the same set of codes, and the same set of visual marker descriptors, but permutes the code assignments across panels. Thus, for every query, the negative document contains the queried code and the queried visual descriptor, but not in the correct local binding. This construction removes easy global cues. Since d_A and d_B contain the same objects, colors, shapes, codes, and document structure, a model cannot solve the task by checking whether the requested elements are present somewhere in the page. It must instead determine whether the code and the visual marker are bound to each other in the same local region. This is precisely the kind of evidence that can be obscured by a single pooled embedding.

We generate 40 document pairs. Each pair contains 25 code–marker bindings, and we create one query for each binding, yielding 1000 queries in total. A query asks for a specific local binding, e.g., "find the report where code x labels the red star marker." For each query, we rank only the

two documents from the same pair: the positive document d_A and the hard negative d_B. We report pairwise accuracy, the fraction of queries for which the scoring function assigns a higher score to d_A than to d_B.

Using only the original single-vector score yields 31.9%. Late interaction alone improves to 56.8%, indicating that non-pooling hidden states retain local binding evidence. The hybrid score improves over the pooled score to 42.6%, but remains below late interaction alone because this adversarial benchmark intentionally makes the pooled global signal misleading. Thus, this probe is intended to isolate local evidence in hidden states rather than to evaluate the default hybrid scoring used in natural retrieval benchmarks.

B Applicable Task Categorization

In this work, we focus our evaluation on dense, corpus-level retrieval tasks (e.g., Image, Visual Document, and Video Retrieval) where the semantic complexity of the query and target necessitates fine-grained alignment. While SoTA single-vector models compress the entire multi-modal representation into a designated token (e.g., `<eot>`), this creates an information bottleneck for complex retrieval. Conversely, SMART leverages late interaction across all hidden states between the query and the corpus, preserving rich, token-level semantics.

We explicitly distinguish these complex retrieval tasks from classification, standard VQA, visual grounding, and temporal localization tasks (particularly in MMEB-V2 [15] that we report on), as they present fundamentally different architectural and definitional challenges:

Classification and VQA: In these tasks, the target is typically a low-entropy concept (e.g., "dog" or "43") that is easily compressed into a single vector. Applying SMART here yields no benefit. Furthermore, forcing dense, token-level interaction on single-label tasks can actively introduce noise, as the model attempts to find complex local alignments where none meaningfully exist.

Visual Grounding (Image): We omit image-based visual grounding due to inherent ambiguities when cast as an open-corpus retrieval problem. In standard grounding, the objective is to localize a specific crop within a *provided* source image. When expanded to a retrieval formulation across a broader corpus, a query for "dog" becomes confounded by valid distractor crops from *other* images. The model is penalized for retrieving semantically correct matches due to these spurious correlations, which does not match the purpose of dense corpus-level retrieval.

Video Moment Retrieval: Finally, while video moment retrieval features a better-defined corpus (e.g., candidate clips isolated within a specific movie), the required semantic granularity from considering groups of tokens mismatches SMART's design. Identifying a dynamic action like "running" requires holistic spatiotemporal abstraction. SMART computes fine-grained, token-by-token similarities and is inference-only, which lacks the explicit temporal reasoning necessary to effectively align high-level, abstract action semantics to singular spatial patches within individual frames. Future work could explore intermediate trainable modules that aggregate temporal continuous features into discrete semantic units, making them amenable to SMART.

Slight Architectural Adjustments for Composed Image Retrieval For Composed Image Retrieval (CIR) benchmarks, spurious correlations [26] persist and negatively affect model performance. Thus, at inference time, we modify SMART for these tasks by masking the query vision tokens to prevent misleading visual alignments and significantly improve overall retrieval accuracy.

C Visualization

Figure 4 shows additional cases where the original single-vector retriever fails but SMART retrieves the correct candidate. These examples illustrate a limitation of relying only on a pooled representation. The single-vector result is often globally plausible, sharing broad visual semantics such as stone buildings, castles, towers, or monastery-like structures, but can miss localized details needed to identify the correct instance. SMART corrects these cases by complementing the pooled score with late interaction over the remaining hidden states, allowing local visual evidence in the query to be matched against corresponding regions in the candidate image.

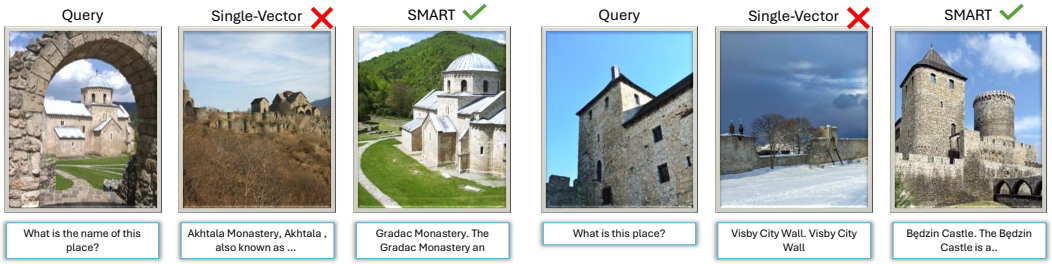

Figure 4: Additional qualitative examples where the original single-vector retriever fails but SMART retrieves the correct candidate. The single-vector model can select images that are globally plausible but miss localized visual evidence, while SMART improves retrieval by adding token-level matching over hidden states.

Figure 5: Token-level visualization of SMART. For selected query image tokens, we show the top-5 candidate-image tokens. The highlighted regions illustrate that SMART's late-interaction score captures localized visual evidence rather than only global image similarity.

Figure 5 further visualizes where this token-level evidence comes from. For each selected query token, we highlight the top-5 candidate-image tokens with the highest hidden-state cosine similarity. The highest-scoring token corresponds to the match used by the MaxSim aggregation in s_{late}, while the remaining high-similarity tokens reveal nearby local evidence supporting the same token-level comparison. The highlighted patches concentrate on semantically meaningful regions, such as towers, roof structures, walls, entrances, and distinctive architectural details, rather than spreading uniformly over the image. This suggests that SMART recovers localized correspondences that can be obscured when the entire image is compressed into a single global embedding.

Table 5: Results of training models with SoTA when evaluated on MMEB-V2's visdoc subset. ✗$_s$ denotes no SMART with single-vector scoring only, while ✗$_m$ denotes no SMART with late-interaction/multi-vector scoring only. ✓denotes SMART hybrid scoring s_{hybrid} and ✓† means LoRA with s_{hybrid}.

Model	**Size**	**SMART**		**Visdoc**				**Average**
		Train	Eval	VDRv1	VDRv2	VR	OOD	
Our Trained Embedders (LamRA-Ret Family)								
LamRA-Single	2B	✗$_s$	✗$_s$	81.58	50.72	78.41	63.50	72.60
LamRA-Single-SMART		✗$_s$	✓	83.02	52.25	50.52	64.50	74.18
LamRA-Multi		✗$_m$	✗$_m$	87.93	54.29	85.24	67.91	78.31
LamRA-Hybrid		✓	✓	**88.14**	**55.81**	**86.39**	**68.90**	**79.10**

D Ablation for Hybrid Scoring

Row 4 of Table 5 further highlights the necessity of our hybrid design. LamRA-Hybrid unites the trained MaxSim interaction with the pooled single-token anchor. This combined approach yields the highest overall performance (79.10), empirically justifying SMART's hybrid scoring design and delivering a 6.5-point average improvement over the original single-vector baseline.

Most notably, **hybrid scoring elevates our LamRA to virtually match the SoTA performance of Qwen3-VL-Embedding-2B** (79.10 vs. 79.27 average). When contrasted with the opaque and likely massive training data and compute budgets utilized by standard SoTA dense embedding models, our results demonstrate that SMART is more than just a powerful inference trick; using it during training also serves as a catalyst, pushing originally weaker models towards further multimodal retrieval capabilities.